

---

# Learning Human Pose Estimation Features with Convolutional Networks

---

**Arjun Jain**  
New York University  
ajain@nyu.edu

Jonathan Tompson  
New York University  
tompson@cims.nyu.edu

Mykhaylo Andriluka  
MPI Saarbruecken  
andrilluk@mpi-inf.mpg.de

Graham W. Taylor  
University of Guelph  
gwtaylor@uoguelph.ca

Christoph Bregler  
New York University  
chris.bregler@nyu.edu

## Abstract

This paper introduces a new architecture for human pose estimation using a multi-layer convolutional network architecture and a modified learning technique that learns low-level features and higher-level weak spatial models. Unconstrained human pose estimation is one of the hardest problems in computer vision, and our new architecture and learning schema shows significant improvement over the current state-of-the-art results. The main contribution of this paper is showing, for the first time, that a specific variation of deep learning is able to outperform all existing traditional architectures on this task. The paper also discusses several lessons learned while researching alternatives, most notably, that it is possible to learn strong low-level feature detectors on features that might even just cover a few pixels in the image. Higher-level spatial models improve somewhat the overall result, but to a much lesser extent than expected. Many researchers previously argued that the kinematic structure and top-down information is crucial for this domain, but with our purely bottom up, and weak spatial model, we could improve other more complicated architectures that currently produce the best results. This mirrors what many other researchers, like those in the speech recognition, object recognition, and other domains have experienced. [24].



Figure 1: Green cross is our new techniques wrist locator, red cross is the state-of-the-art CVPR13 MODEC detector on the FLIC database.

## 1 Introduction

One of the hardest tasks in computer vision is determining the high degree of freedom configuration of a human body with all its limbs, complex self occlusion, self-similar parts, and large variations due to clothing, body-type, lighting, and many other factors. The most challenging scenario for this problem is from a monocular RGB image and with no prior assumptions made using motion models, pose models, background models, or any other common heuristics that current state-of-the-art systems utilize. Finding a face in frontal or side view is relative simple, but determining the

exact location of body parts such as hands, elbows, shoulders, hips, knees and feet, each of which sometimes only occupying a few pixels in the image in front of an arbitrary cluttered background, is significantly harder.

The best performing pose estimation methods, including those based on deformable part models, typically are based on body part detectors. Such body part detectors commonly consist of multiple stages of processing. The first stage of processing in a typical pipeline consists of extracting sets of low-level features such as SIFT [23], HoG [10], or other filters that describe orientation statistics in local image patches. Next, these features are pooled over local spatial regions and sometimes across multiple scales to reduce the size of the representation and also develop local shift/scale invariance. Finally, the aggregate features are mapped to a vector, which is then either input to 1) a standard classifier such as a support vector machine (SVM) or 2) the next stage of processing (e.g. assembling the parts into a whole). Much work is devoted to engineering the system to produce a vector representation that is sensitive to class (e.g. head, hands, torso) while remaining invariant to the various nuisance factors (lighting, viewpoint, scale, etc.)

An alternative approach is *representation learning*: relying on the data instead of feature engineering, is to *learn* a good representation, in this case one that is invariant to nuisance factors. For a recent review, see [6]. It is common to learn multiple layers of representation, which is referred to as *deep learning*. Several such techniques have used unsupervised or semi-supervised learning to extract multi-layer domain-specific invariant representations, however, it is purely supervised techniques that have won several recent challenges, including ImageNet LSVRC 2012 by a large margin [21]. These end-to-end learning systems have capitalized on advances in computing hardware (notably GPUs), larger datasets like ImageNet, and algorithmic advances (specifically gradient-based training methods and regularization).

While these methods are now proven in generic object recognition, their use in pose estimation has been limited. Part of the challenge in making end-to-end learning work for human pose estimation is related to the nonrigid structure of the body, the necessity for precision (deep recognition systems often throw away precise location information through pooling), and the complex, multi-modal nature of pose.

In this paper, we present the first end-to-end learning approach for full-body human pose estimation. While our approach is based on convolutional networks (convnets) [22], we want to stress that the naïve implementation of applying this model “off-the-shelf” will not work. Therefore, the contribution of this work is in both a model that outperforms state of the art deformable part models (DPMs) on a modern, challenging dataset, and also an analysis of what is needed to make convnets work in human pose estimation. In particular, we present a two-stage filtering approach whereby the response maps of convnet part detectors are denoised by a second process informed by the part hierarchy.

## 2 Related Work

Detecting people and their pose has been investigated for decades. Many early techniques rely on sliding-window part detectors based on hand crafted or learned features or silhouette extraction techniques applied to controlled recording conditions. Examples include [14, 44, 5, 27]. We refer to [30] for a complete survey of this era. More recently, several new approaches have been proposed, that are applied to unconstrained domains. In such domains, good performance has been achieved with so called bag of features followed by regression-based, nearest neighbor or SVM based architectures. Examples include “shape-context” edge based histograms from the human body [26, 1] or just silhouette features [19]. Shakhnarovich et al. [34] use HOG [11] features and boosting for learning a parameter sensitive hash function. Many relevant techniques have also been applied to hand tracking such as [43]. A more general survey of the large field of hand tracking can be found at [12].

Many techniques have been proposed that extract, learn, or reason over entire body features. Some use a combination of local detectors and structural reasoning (see [31] for coarse tracking and [9] for person-dependent tracking). In a similar spirit, more general techniques using pictorial structures [2, 3, 17, 32], “poselets” [8], and other part-models [15, 45] have received increased attention. We will focus on these techniques and their latest incarnations further below in various sections.

Also related to our approach is Shotton’s et al Kinect based body part detector [35] that uses a random forest of decision trees, that is trained on simple body part detectors.

Further examples come from the HumanEva dataset competitions [36], or approaches that use higher-resolution shape models such as SCAPE [4] and further extensions [20, 7]. These differ from our domain in that the images considered are of higher quality and less cluttered. Also many of these techniques work on single camera, but need video sequence input (not single images) to achieve impressive results [37, 46].

There are a number of successful end-to-end representation learning techniques which perform pose estimation on a limited subset of body parts. One of the earliest examples of this type was Nowlan and Platt’s convolutional neural network hand tracker [27], which tracked a single hand. Osadchy et al. applied a convolutional network to simultaneously detect and estimate the pitch, yaw and roll of a face [28]. Taylor et al. [39] trained a convolutional neural network to learn an embedding in which images of people in similar pose lie nearby. They used a subset of body parts, namely, the head and hand locations to learn the “gist” of a pose, and resorted to nearest-neighbour matching rather than explicitly modeling pose. Perhaps most relevant to our work is Taylor et al.’s work on tracking people in video [40], augmenting a particle filter with a structured prior over human pose and dynamics based on learning representations. While they estimated a posterior over the whole body (60 joint angles), their experiments were limited to the HumanEva dataset [36], which was collected in a controlled laboratory setting. The datasets we consider in our experiments are truly poses “in the wild”, though we do not consider dynamics.

A factor limiting earlier methods from tackling full pose-estimation with end-to-end learning methods, in particular deep networks, was the limited amount of labeled data. Such techniques, with millions or more parameters, require more data than structured techniques that have more *a priori* knowledge, such as DPMs. We attack this issue on two fronts. First, directly, by using larger labeled training sets which have become available in the past year or two, such as FLIC [33]. Second, indirectly, by better exploiting the data we have. The annotations provided by typical pose estimation datasets contain much richer information compared to the class labels in object recognition datasets. In particular, we show that the relationships among parts contained in these annotations can be used to build better detectors.

### 3 Model

To perform pose estimation with a convolutional network architecture [22] (convnet), the most obvious approach would be to map the image input directly to a vector coding the articulated pose: i.e. the type of labels found in pose datasets. The convnet output would then be linear and unbounded, representing 2-D or 3-D positions of joints, or a hierarchy of joint angles. However, we found that this worked very poorly. One issue is that pooling, while useful for improving translation invariance during object recognition, destroys precise spatial information which is necessary to accurately predict pose. Convnets that produce segmentation maps, for example, avoid pooling completely [42, 13]. Another issue is that the direct mapping from input space to kinematic body pose coefficients is highly non-linear and not one-to-one. However, even if we took this route, there is a deeper issue with attempting to map directly to a representation of full body pose. Valid poses represent a much lower-dimensional manifold in the high-dimensional space in which they are captured. It seems troublesome to make a discriminative network map to a space in which the majority of configurations do not represent valid poses. In other words, it makes sense to restrict the net’s output to a much smaller class of valid configurations.

Rather than perform multi-class classification using a single convnet to learn pose coefficients directly, we found that training multiple convnets to perform independent binary body-part classification, with one network per feature, results in improved performance on our dataset. These convnets are applied as *sliding windows* to overlapping regions of the input, and map a window of pixels to a single binary output: the presence or absence of that body part. The result of applying the convnet is a response map indicating the confidence of the body part at that location. This lets us use much smaller convnets, and retain the advantages of pooling, at the expense of having to maintain a separate set of parameters for each body part. Of course, a series of independent part detectors cannot enforce consistency in pose in the same way as a structured output model, which produces valid full-

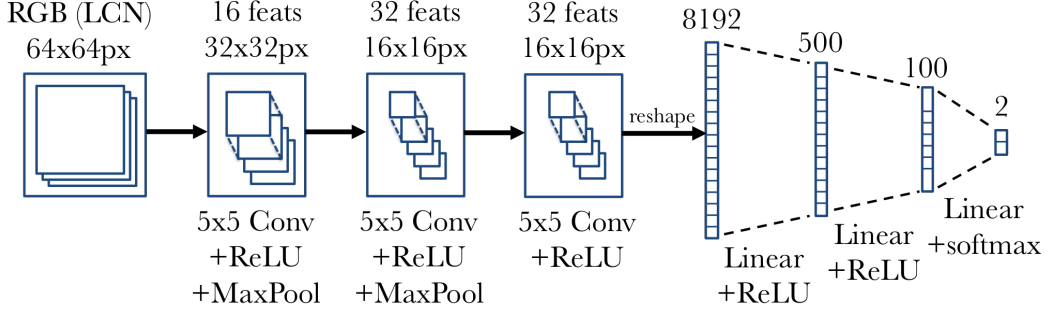


Figure 2: Convolutional Network

body configurations. In the following sections, we first describe in detail the convolutional network architecture and then a method of enforcing pose consistency using parent-child relationships.

### 3.1 Convolutional Network Architecture

The lowest level of our feature detection pipeline is based on a standard convnet architecture, an overview of which is shown in Figure 2. Convnets, like their fully-connected, deep neural network counterparts, perform end-to-end feature learning and are trained with the back-propagation algorithm. However, they differ in a number of respects, most notably local connectivity, weight sharing, and local pooling. The first two properties significantly reduce the number of free parameters, and reduce the need to learn repeated feature detectors at different locations of the input. The third property makes the learned representation invariant to small translations of the input.

The convnet pipeline shown in Figure 2 starts with a  $64 \times 64$  pixel RGB input patch which has been local contrast normalized (LCN) to emphasize geometry discontinuities and improve generalization performance [29]. The three channel input is then fed through three convolution and subsampling layers, and is finally followed by a three-stage fully-connected neural network to perform the final per-patch classification.

In each of the three stages of convolution and pooling, as shown in Figure 2, the pooled output from layer  $l - 1$ ,  $\mathbf{y}^{l-1}$ , is convolved with a series of learned filters  $\mathbf{k}^l$  and summed to produce *feature maps*  $\mathbf{x}^l$ . These are subsequently pooled using a downsampling operator with factor  $s$  to produce pooled map  $\mathbf{y}^l$ . This can be represented mathematically as:

$$\mathbf{x}_j^l = f \left( \sum_{i \in M_j} \mathbf{y}_i^{l-1} * \mathbf{k}_{ij}^l + b_j^l \right) \quad (1)$$

$$\mathbf{y}_j^l = \beta_j^l \text{down}(\mathbf{x}_j^l, s) \quad (2)$$

where  $b$  and  $\beta$  are additive and multiplicative learned coefficients. Note that every map in layer  $l - 1$  need not be connected to every map in layer  $l$ . Therefore  $M_j$  is an index, representing the set of maps in layer  $l - 1$  to which feature  $j$  in layer  $l$  is connected via filter  $\mathbf{k}_{ij}$ . The function  $f$  is an element-wise nonlinearity, often a sigmoid or tanh operator. In our experiments, we use rectified linear units (ReLUs) [18]:

$$f(x) = \begin{cases} x & \text{if } x > 0 \\ 0 & \text{otherwise} \end{cases} \quad (3)$$

The feature maps at layer 0,  $\mathbf{y}^0$ , represent the input image where the individual channels,  $i$ , are colors.

Following the three stages of convolution and subsampling (Eqs 1-2) the top-level pooled map  $\mathbf{y}$  is flattened to a vector and processed by three *fully connected* layers, analogous to those used in

deep neural networks. The final layer is the *output layer* and its form is determined by the quantity to predict. For example, in multi-class classification, where convnets are most typically used, the output layer uses a *softmax* function whose output can be interpreted as probabilities over classes.

To train the convent, we perform standard batched stochastic gradient descent. Of the training set images, we used a validation set to hand tune the network hyper-parameters, such as number and size of features, learning rate, momentum coefficient, etc. Section 4 contains more details on the specific parameters we experimented with. We use Nesterov momentum [38] as well as RMSPROP [41] to decrease training time and we use L2 regularization and dropout [21] on the input to each of the fully-connected linear stages to reduce overfitting on our restricted size training set.

We also adopt an approach popular in the detection community, that is, mining hard negative examples [16]. Every 50 epochs, we run the current model on all negatives of the training set ( $\approx 400,000$  negatives). All negatives which are correctly classified with a confidence greater than 0.99 are marked as *weak* negatives, which are excluded from the training set. During subsequent mining iterations, the set of *weak* negatives are also checked if they still can be classified correctly with high confidence failing which they are added back to the training set.

### 3.2 Enforcing pose consistency through two-stage filtering

We believe that due to the small and constraining image context as input to the convolutional network (64x64 pixels) and limited training set size, we get many false positives on the test set. We therefore use a higher-level graphical model with simple priors to remove outliers. We start with a global position prior for the face, which is obtained by first creating a histogram over the face positions in the training images, as shown in Figure 3.2(a). Figure 3.2(b) shows the smooth version of this histogram  $h(\text{face})$  which we then use to weight the output confidence of the face detector  $op(\text{face})$ . In log space, the weighted output confidence  $conf(\text{face}) = h(\text{face}) + \lambda op(\text{face})$ , where  $\lambda$  is a mixing parameter.

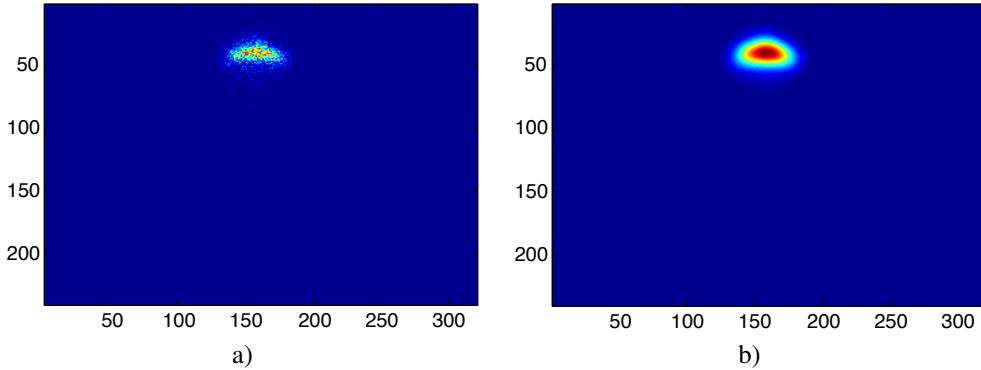


Figure 3: Global priors for face: a) histogram of face positions from training images, b) smoothened histogram

The final face position is then the location that corresponds to the maximum value in  $conf(\text{face})$ .

We also create 3 other histograms:  $h(\text{shoulder}/\text{face})$ ,  $h(\text{elbow}/\text{shoulder})$ ,  $h(\text{wrist}/\text{elbow})$  as shown in fig. 3.2. For example,  $h(\text{wrist}/\text{elbow})$  is a histogram for the wrist positions if the elbow was at the centre. Note how  $h(\text{elbow}/\text{wrist})$ , etc are a 180 degree rotation of  $h(\text{wrist}/\text{elbow})$ .

Using these, we can propagate the face evidence to the shoulder in a convolution setting as:  $conf(\text{shoulder}) = conf(\text{face}) * h(\text{shoulder}/\text{face}) + \lambda op(\text{shoulder})$  and similarly for others. Note how this convolution is mathematically equivalent to the sum-product algorithm in belief-propagation. In the future, we want to learn these filters jointly such that we can learn the mixing weight as well as have better priors.

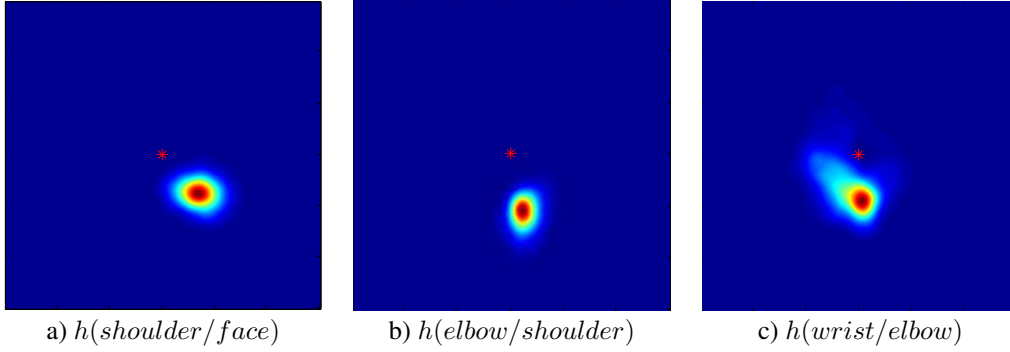


Figure 4: Part priors

## 4 Results

Here we present results on the FLIC[33] dataset. We use 3987 training images from the dataset which we also flip to get  $3987 \times 2 = 7974$  examples. Since the training images are not the same scale, we also manually annotate the bounding box for the head in these images, and bring them to canonical scale. Further, we crop them to  $320 \times 240$  such that the centre of the shoulder annotations lies at (160 px, 80 px). For testing, of the 1016 test examples, we only run our model on images with only one person (351 images). We run it on 6 scales and perform a non-maximal suppression to combine the results from all the scales.

We use Theano. While training, for optimal GPU memory usage, we only keep 100 mini-batches on the GPU. This allows us to use bigger models, and does not constraint us with the size of training data that we can use. Our system has two main threads of execution: 1) training function which runs on the GPU, and 2) data dispatch function which preprocesses the data on the cpu and transfers it on the GPU when thread 1) is finished processing the 100 mini batches. Training on NVIDIA TITAN GPU's take 4 hours.

For testing, because of the shared nature of weights for all windows of the images, we convolve the learnt filters with the full image instead of individual windows. This makes our testing pipe line much faster and it us takes 20 ms per image. Our spatial model also runs of the GPU using Theano. We run the spatial model over all the scales and then perform non-maximal suppression.

In fig. 4 we present results for the body parts wrist, elbow and shoulder. We also compare our detector to DPM and MODEC. As noted earlier, we do not improve much with the spatial model.



Figure 5: Learnt  $5 \times 5 \times 3$  first layer filters for the wrist detector.

## 5 Conclusion

We have shown successfully how to improve the state-of-the-art on one of the most complex computer vision tasks, the unconstrained human pose estimation. The surprising discovery presented in this paper includes, we were able to learn very strong low-level feature detectors that by itself are already very impressive, and out-perform many popular and more complex model. We explored many different higher level structural models with the aim to further improve the results, but the most generic higher level spatial model achieved the best results. As mentioned at the beginning, this is counter intuitive to common believe for human kinematic structures, but it mirrors results in



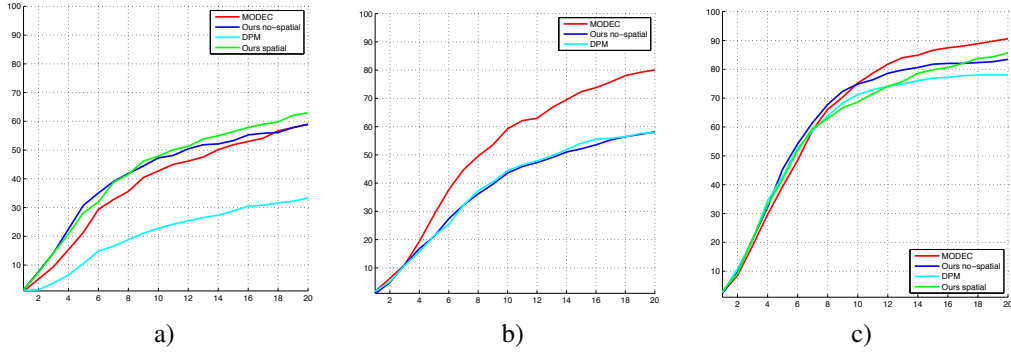


Figure 6: Detector comparisons for a) Wrist, b) Elbow, and c) Shoulder on the 351 image subset.



Figure 7: Failure cases: Green cross is our new techniques wrist locator, red cross is the state-of-the-art CVPR13 MODEC detector on the FLIC database.

other domains. For instance in speech recognition, researchers observed, if the learned transition probabilities (higher level structure) are reset to equal probabilities, the recognition performance, now mainly driven by the emission probabilities does not reduce significantly [25]. Other domains are discussed in more details by [24].

We expect to get further improvement of our model in enlarging the training set with a new pose-based warping technique that we are currently investigating (and plan to update in a few weeks for this ICLR2014 submission). Furthermore, we are also currently experimenting with multi-resolution input representations, that take a larger spatial context into account. Again, we plan to update in a few weeks this ICLR2014 submission with new results.

## 6 Acknowledgement

This research was funded in part by the Office of Naval Research ONR Award N000141210327 and by a google award.

## References

- [1] A. Agarwal, B. Triggs, I. Rhone-Alpes, and F. Montbonnot. Recovering 3D human pose from monocular images. *IEEE Transactions on Pattern Analysis and Machine Intelligence*, 28(1):44–58, 2006. 2
- [2] M. Andriluka, S. Roth, and B. Schiele. Pictorial structures revisited: People detection and articulated pose estimation. In *CVPR*, 2009. 2
- [3] M. Andriluka, S. Roth, and B. Schiele. Monocular 3d pose estimation and tracking by detection. In *Computer Vision and Pattern Recognition (CVPR), 2010 IEEE Conference on*, pages 623–630. IEEE, 2010. 2
- [4] D. Anguelov, P. Srinivasan, D. Koller, S. Thrun, J. Rodgers, and J. Davis. Scape: shape completion and animation of people. In *ACM Transactions on Graphics (TOG)*, volume 24, pages 408–416. ACM, 2005. 3
- [5] V. Athitsos, J. Alon, S. Sclaroff, and G. Kollias. Boostmap: A method for efficient approximate similarity rankings. *CVPR*, 2004. 2

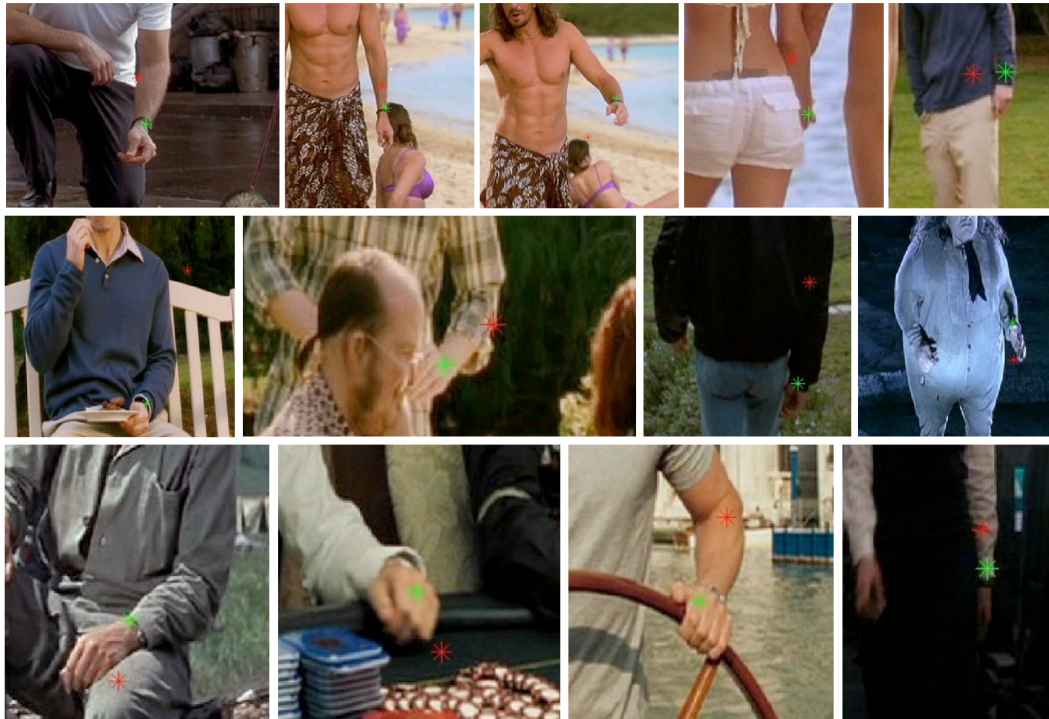


Figure 8: Success cases: Green cross is our new techniques wrist locator, red cross is the state-of-the-art CVPR13 MODEC detector on the FLIC database.

- [6] Y. Bengio, A. C. Courville, and P. Vincent. Representation learning: A review and new perspectives. Technical report, University of Montreal, 2012. 2
- [7] M. Black, D. Hirshberg, M. Loper, E. Rachlin, and A. Weiss. Co-registration – simultaneous alignment and modeling of articulated 3D shapes. European patent application EP12187467.1 and US Provisional Application, Oct. 2012. 3
- [8] L. Bourdev and J. Malik. Poselets: Body part detectors trained using 3d human pose annotations. In *ICCV*, sep 2009. 2
- [9] P. Buehler, A. Zisserman, and M. Everingham. Learning sign language by watching TV (using weakly aligned subtitles). *CVPR*, 2009. 2
- [10] N. Dalal and B. Triggs. Histograms of oriented gradients for human detection. In *Computer Vision and Pattern Recognition, 2005. CVPR 2005. IEEE Computer Society Conference on*, volume 1, pages 886–893. IEEE, 2005. 2
- [11] N. Dalal, B. Triggs, and C. Schmid. Human detection using oriented histograms of flow and appearance. *ECCV*, 2006. 2
- [12] A. Erol, G. Bebis, M. Nicolescu, R. D. Boyle, and X. Twombly. Vision-based hand pose estimation: A review. *Computer Vision and Image Understanding*, 108(1):52–73, 2007. 2
- [13] C. Farabet, C. Couprie, L. Najman, and Y. LeCun. Scene parsing with multiscale feature learning, purity trees, and optimal covers. In *ICML*, 2012. 3
- [14] A. Farhadi, D. Forsyth, and R. White. Transfer Learning in Sign language. In *CVPR*, 2007. 2
- [15] P. Felzenszwalb, D. McAllester, and D. Ramanan. A discriminatively trained, multiscale, deformable part model. In *CVPR*, 2008. 2
- [16] P. F. Felzenszwalb, R. B. Girshick, D. McAllester, and D. Ramanan. Object detection with discriminatively trained part-based models. *PAMI'10*. 5
- [17] V. Ferrari, M. Marin-Jimenez, and A. Zisserman. Pose search: Retrieving people using their pose. In *CVPR*, 2009. 2
- [18] X. Glorot, A. Bordes, and Y. Bengio. Deep sparse rectifier networks. In *Proceedings of the 14th International Conference on Artificial Intelligence and Statistics. JMLR W&CP Volume*, volume 15, pages 315–323, 2011. 4
- [19] K. Grauman, G. Shakhnarovich, and T. Darrell. Inferring 3d structure with a statistical image-based shape model. In *ICCV*, pages 641–648, 2003. 2



- [20] N. Hasler, C. Stoll, M. Sunkel, B. Rosenhahn, and H.-P. Seidel. A statistical model of human pose and body shape. In P. Dutré and M. Stamminger, editors, *Computer Graphics Forum (Proc. Eurographics 2008)*, volume 2, Munich, Germany, Mar. 2009. 3
- [21] A. Krizhevsky, I. Sutskever, and G. Hinton. Imagenet classification with deep convolutional neural networks. In *Advances in Neural Information Processing Systems 25*, pages 1106–1114, 2012. 2, 5
- [22] Y. LeCun, L. Bottou, Y. Bengio, and P. Haffner. Gradient-based learning applied to document recognition. *Proc. IEEE*, 86(11):2278–2324, 1998. 2, 3
- [23] D. G. Lowe. Object recognition from local scale-invariant features. In *Computer vision, 1999. The proceedings of the seventh IEEE international conference on*, volume 2, pages 1150–1157. Ieee, 1999. 2
- [24] A. Lucchi, Y. Li, X. Boix, K. Smith, and P. Fua. Are spatial and global constraints really necessary for segmentation? In *Computer Vision (ICCV), 2011 IEEE International Conference on*, pages 9–16. IEEE, 2011. 1, 7
- [25] N. Morgan. personal communication. 7
- [26] G. Mori and J. Malik. Estimating human body configurations using shape context matching. *ECCV*, 2002. 2
- [27] S. J. Nowlan and J. C. Platt. A convolutional neural network hand tracker. *Advances in Neural Information Processing Systems*, pages 901–908, 1995. 2, 3
- [28] M. Osadchy, Y. L. Cun, and M. L. Miller. Synergistic face detection and pose estimation with energy-based models. *The Journal of Machine Learning Research*, 8:1197–1215, 2007. 3
- [29] N. Pinto, D. D. Cox, and J. J. DiCarlo. Why is real-world visual object recognition hard? *PLoS computational biology*, 4(1):e27, 2008. 4
- [30] R. Poppe. Vision-based human motion analysis: An overview. *Computer Vision and Image Understanding*, 108(1-2):4–18, 2007. 2
- [31] D. Ramanan, D. Forsyth, and A. Zisserman. Strike a pose: Tracking people by finding stylized poses. In *CVPR*, 2005. 2
- [32] B. Sapp, C. Jordan, and B. Taskar. Adaptive pose priors for pictorial structures. In *CVPR*, 2010. 2
- [33] B. Sapp and B. Taskar. Multimodal decomposable models for human pose estimation. In *CVPR'13*. 3, 6
- [34] G. Shakhnarovich, P. Viola, and T. Darrell. Fast pose estimation with parameter-sensitive hashing. In *ICCV*, pages 750–759, 2003. 2
- [35] J. Shotton, T. Sharp, A. Kipman, A. Fitzgibbon, M. Finocchio, A. Blake, M. Cook, and R. Moore. Real-time human pose recognition in parts from single depth images. *Communications of the ACM*, 56(1):116–124, 2013. 3
- [36] L. Sigal, A. Balan, and B. M. J. HumanEva: Synchronized video and motion capture dataset and baseline algorithm for evaluation of articulated human motion. *IJCV*, 87(1/2):4–27, 2010. 3
- [37] C. Stoll, N. Hasler, J. Gall, H. Seidel, and C. Theobalt. Fast articulated motion tracking using a sums of gaussians body model. In *Computer Vision (ICCV), 2011 IEEE International Conference on*, pages 951–958. IEEE, 2011. 3
- [38] I. Sutskever, J. Martens, G. Dahl, and G. Hinton. On the importance of initialization and momentum in deep learning. 5
- [39] G. Taylor, R. Fergus, I. Spiro, G. Williams, and C. Bregler. Pose-sensitive embedding by nonlinear NCA regression. In *Advances in Neural Information Processing Systems 23 (NIPS)*, pages 2280–2288, 2010. 3
- [40] G. Taylor, L. Sigal, D. Fleet, and G. Hinton. Dynamical binary latent variable models for 3d human pose tracking. In *Proc. of the 23rd IEEE Computer Society Conference on Computer Vision and Pattern Recognition (CVPR)*, 2010. 3
- [41] T. Tieleman and G. Hinton. Lecture 6.5-rmsprop: Divide the gradient by a running average of its recent magnitude. *COURSERA: Neural Networks for Machine Learning*, 2012. 5
- [42] S. C. Turaga, J. F. Murray, V. Jain, F. Roth, M. Helmstaedter, K. Briggman, W. Denk, and H. S. Seung. Convolutional networks can learn to generate affinity graphs for image segmentation. *Neural Computation*, 22:511–538, 2010. 3
- [43] R. Y. Wang and J. Popović. Real-time hand-tracking with a color glove. In *ACM Transactions on Graphics (TOG)*, volume 28, page 63. ACM, 2009. 2
- [44] C. Wren, A. Azarbayejani, T. Darrell, and A. Pentland. Pfinder: Real-time tracking of the human body. *IEEE Transactions on Pattern Analysis and Machine Intelligence*, 19(7):780–785, 1997. 2
- [45] Y. Yang and D. Ramanan. Articulated pose estimation with flexible mixtures-of-parts. In *Computer Vision and Pattern Recognition (CVPR), 2011 IEEE Conference on*, pages 1385–1392. IEEE, 2011. 2
- [46] S. Zuffi, J. Romero, C. Schmid, and M. J. Black. Estimating human pose with flowing puppets. 3